EPSC2018

SB2 abstracts

EPSC Abstracts
Vol. 12, EPSC2018-135, 2018
European Planetary Science Congress 2018

ESO/VLT/SPHERE Survey of D>100km Asteroids (2017-2019): First Results

P. Vernazza (1), M. Marsset (2), J. Hanus (3), B. Carry (4), M. Viikinkoski (5), A. Drouard (1), R. Fetick (1), F. Marchis (6), E. Podlewska (7), P. Bartczak (7), T. Santana-Ros (7), M. Birlan (8), C. Dumas (9), M. Kaasalainen (5), B. Yang (10), J. Durech (3), L. Jorda (1), P. Lamy (1), A. Vigan (1), T. Fusco (1), T. Michalowski (7), A. Marciniak (7), M. Pajuelo (8), P. Michel (4), P. Tanga (4), J. Berthier (8), F. Vachier (8), J. Castillo-Rogez (11), O. Witasse (12), F.Cipriani (12), E. Jehin (13), M. Ferrais (13)

(1) Laboratoire d'Astrophysique de Marseille, France, (pierre.vernazza@lam.fr / Phone: +33-4-91055911) (2) Queen's University of Belfast, UK (3) Charles University in Prague, CZ (4) OCA, France (5) TUT, Finland (6) Seti institute, USA (7) Astronomical Observatory Institute, Faculty of Physics, Adam Mickiewicz University, PL (8) IMCCE, FR, (9) TMT, USA, (10) ESO, CL, (11) JPL, USA, (12) ESTEC, NL, (13) Institut d'Astrophysique de l'Université de Liège , BE

Abstract

The vast majority of the geological constraints (i.e., internal structure via the density, cratering history) for main belt asteroids have so far been obtained via dedicated interplanetary missions (e.g., Rosetta, DAWN). The high angular resolution of SPHERE/ZIMPOL (one pixel represents 3.6 x 3.6 mas on sky), the new-generation visible adaptive-optics camera at ESO/VLT, implies that such science objective can now be investigated from the ground for a large fraction of D≥100 km main-belt asteroids (most of these bodies possess an angular diameter around opposition larger than 100 mas). The sharp images acquired by this instrument can be used to constrain accurately the shape and thus volume of these bodies (hence density when combined with mass estimates) and to characterize the distribution and topography of D≥30 km craters across their surfaces.

To make substantial progress in our understanding of the shape, internal compositional structure (i.e., density) and surface topography of large main belt asteroids, we are carrying out an imaging survey via an ESO Large program entirely performed in service mode with seeing constraints <0.8" (152h in total; PI: P. Vernazza; ID: 199.C-0074; the observations are spread over 4 semesters from April 1st, 2017 till March 30, 2019) of a statistically significant fraction of all D>100 km main-belt asteroids (~35 out of ~200 asteroids; our survey covers the major compositional classes) at high angular-resolution with VLT/SPHERE throughout their rotation (typically 6 epochs per target).

Here, we will present a summary of the results obtained after one year of observations.

EPSC Abstracts
Vol. 12, EPSC2018-144, 2018
European Planetary Science Congress 2018

New insights into Pallas' formation and collisional history from VLT/SPHERE and SOFIA/FORCAST

M. Marsset (1), P. Vernazza (2) J. Hanuš (3), M. Viikinkoski (4), B. Carry (5), A. Drouard (2), R. Fetick (2), F. Marchis (6), E. Podlewska (7), P. Bartczak (7), T. Santana-Ros (7), M. Birlan (8), C. Dumas (9), M. Kaasalainen (5), B. Yang (10), J. Durech (3), L. Jorda (2), P. Lamy (2), A. Vigan (2), T. Fusco (2), T. Michalowski (7), A. Marciniak (7), M. Pajuelo (8), P. Michel (4), P. Tanga (4), J. Berthier (8), F. Vachier (8), J. Castillo-Rogez (11), O. Witasse (12), F.Cipriani (12), E. Jehin (13), M. Ferrais (13)

(1) Queen's University of Belfast, UK, (michael.marsset@qub.ac.uk / Phone: +44-7-491552511) (2) Laboratoire d'Astrophysique de Marseille, France (3) Charles University in Prague, CZ (4) TUT, Finland (5) OCA, France (6) Seti institute, USA (7) Astronomical Observatory Institute, Faculty of Physics, Adam Mickiewicz University, PL (8) IMCCE, FR, (9) TMT, USA, (10) ESO, CL, (11) JPL, USA, (12) ESTEC, NL, (13) Institut d'Astrophysique de l'Université de Liège , BE

1. Introduction

Large (D>100 km) asteroids are the most direct remnants of the building blocks of planets. With a diameter of ∼510-540 km (Schmidt et al. 2009, Carry et al. 2010), Pallas is the second or third largest object in the asteroid belt and the parent body of a small collisional family. Its spectral properties in the visible and near-infrared indicate a B-type surface (DeMeo et al. 2009), meaning Pallas is most likely linked to carbonaceous chondrite meteorites. Disc-resolved images of Pallas have revealed a nearly hydrostatic shape overprinted by long-wavelength concavities (Schmidt et al. 2009, Carry et al. 2010). This was interpreted as evidence for an early phase of internal heating subsequent to Pallas's formation, followed by several cratering impacts (Schmidt & Castillo-Rogez 2012). The two most recent estimates of Pallas' density, 2.40±0.25 (Schmidt et al. 2009) and 3.40±0.90 (Carry et al. 2010), are rather inconsistent and prevent from differentiating between the various models proposed for its internal structure (Schmidt & Castillo-Rogez 2012). This currently limits our understanding of the formation and early thermal evolution of Pallas.

2. Observations

We report new high-angular resolution observations of (2) Pallas collected in the frame of the SPHERE large survey of the asteroid belt (see Talk by P. Vernazza) with the adaptive-optics-fed SPHERE+ZIMPOL camera on the Very Large Telescope (VLT). A total of 40 images acquired at 8 different epochs provide a full longitudinal coverage of the surface of Pallas. We also present new mid-infrared (∼10-30 micron) spectra of Pallas collected with FORCAST on the Stratospheric Observatory for Infrared Astronomy (SOFIA).

3. Results

Pallas was resolved with ZIMPOL with around ∼120 pixels along the longest axis. The optimal angular resolution of each image was restored with Mistral (Fusco et al. 2002), a myopic deconvolution algorithm optimised for images with sharp boundaries, which allows the identification of many craters and geological features at the surface of Pallas. A precise 3D-shape reconstruction was achieved with the ADAM software (Viikinkoski et al. 2015), providing a high precision estimate of Pallas's volume and hence density. Finally, the FORCAST data was used to search for meteoritic analogs in the mid-infrared. We will present our results and discuss the implications for Pallas's early thermal and collisional evolution.

References

[1] Carry et al. 2010: Physical properties of (2) Pallas, Icarus, 205, 460

[2] DeMeo et al. 2009: An extension of the Bus asteroid taxonomy into the near-infrared, Icarus, 202, 160

[3] Fusco et al. 2002: Deconvolution of astronomical images obtained from ground-based telescopes with adaptive optics, SPIE, 4839, 1065

[4] Schmidt et al. 2009: The Shape and Surface Variation of 2 Pallas from the Hubble Space Telescope, Science, 326, 275

[5] Schmidt & Castillo-Rogez: Water, heat, bombardment: The evolution and current state of (2) Pallas, Icarus, 218, 478

[6] Viikinkoski et al. 2015: ADAM: a general method for using various data types in asteroid reconstruction, A&A, 576, A8

EPSC Abstracts
Vol. 12, EPSC2018-153-2, 2018
European Planetary Science Congress 2018

ESO/VLT/SPHERE Survey of D>100km Asteroids (2017-2019): (7) Iris

J. Hanuš (1), P. Vernazza (2), M. Marsset (3), B. Carry (4), M. Viikinkoski (5), A. Drouard (2), R. Fetick (2), F. Marchis (6), E. Podlewska (7), P. Bartczak (7), T. Santana-Ros (7), M. Birlan (8), C. Dumas (9), M. Kaasalainen (5), B. Yang (10), J. Ďurech (1), L. Jorda (2), P. Lamy (2), A. Vigan (2), T. Fusco (2), T. Michalowski (7), A. Marciniak (7), M. Pajuelo (8), P. Michel (4), P. Tanga (4), J. Berthier (8), F. Vachier (8), J. Castillo-Rogez (11), O. Witasse (12), F. Cipriani (12), E. Jehin (13), M. Ferrais (13)

(1) Astronomical Institute, Faculty of Mathematics and Physics, Charles University in Prague, V Holešovičkách 2, 18000 Prague, CZ (hanus.home@gmail.com) (2) Laboratoire d'Astrophysique de Marseille, France (3) Queen's University of Belfast, UK (4) OCA, France (5) TUT, Finland (6) SETI Institute, CA, USA (7) Astronomical Observatory Institute, Faculty of Physics, Adam Mickiewicz University, PL (8) IMCCE, FR (9) TMT, USA (10) ESO, CL (11) JPL, USA (12) ESTEC, NL (13) Institut d'Astrophysique de l'Université de Liége, BE

Abstract

The high angular resolution of the new-generation visible adaptive-optics camera SPHERE/ZIMPOL mounted on the ESO/VLT telescope on Cerro Paranal opened only recently an exciting opportunity to study asteroid topography and shapes in great details with the ground-based observations [V18]. Such task was so far possible only for the two largest asteroids – (1) Ceres and (4) Vesta. ZIMPOL observations with a pixel scale of 3.6 mas [S17] are about four times sharper than those from the HST (FGS instrument), therefore the instrument is capable of resolving the majority of $D > 100$ km main-belt asteroids, which usually have an angular diameter larger than 100 mas during their convenient apparitions. Currently, only in-situ observations by space probes can provide better images.

In 2016, ESO approved a Large program (PI: P. Vernazza; ID: 199.C-0074) that involves acquiring high angular images of ∼40 asteroids larger than 100 km throughout their rotation during four semesters (starting April 2017). The aim of the observing campaign is to better understand asteroid shapes, their internal composition and local surface topography. Here, we draw our attention to the main-belt asteroid (7) Iris (hereafter simply Iris), which belongs to one of the three largest members of the S-type spectral class.

Five epochs of Iris well spaced in the rotation phase were observed with the SPHERE instrument [B08] during two consecutive nights in October 2017. We clearly resolved several surface features (impact basins) that are consistent throughout the deconvolved images obtained using an modified MISTRAL algorithm with a library set of PSF frames [F03]. The observations are exclusively limited to the south pole of Iris (aspect angle ∼160°) due to the pole-on observing geometry. We compare our shape model to the independent shape model based on delay-Doppler radar data acquired at a similar observing geometry [O10].

The spectacular quality of the images is partly given by the large angular size of Iris – 0.33". Considering the large size of Iris (∼215 km), one pixel represents ∼2.3 km at distance of Iris (0.89 au), which allows us to reliably detect surface details as large as ∼30 km.

We present a scaled-in-size 3D shape model with local topography of Iris (Fig. 1) derived by the All-Data Asteroid Modeling (ADAM) algorithm [V15,V16] that takes both optical lightcurves and disk-resolved images into consideration. Moreover, we also estimate Iris' bulk density. We further comment on the global and local features of Iris' shape with respect to its early and recent collisional history. Finally, we also re-examine the existence of a potential collisional family related to Iris in a search for a possible link with any of the large basins on its surface.

Acknowledgements

JH and JD were supported by the grant 18-09470S of the Czech Science Foundation. This work has been supported by Charles University Research program No. UNCE/SCI/023.

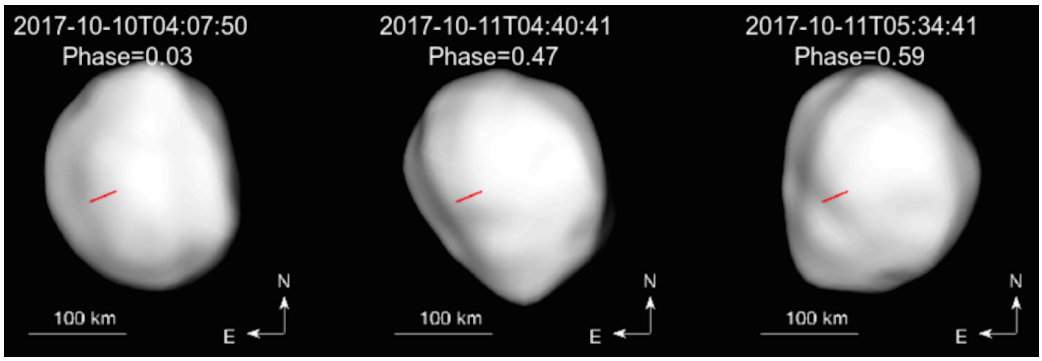

Figure 1: A low-resolution shape model of Iris reconstructed from the optical lightcurves and VLT/SPHERE images. The red line indicates the position of the spin axis with the ecliptic longitude $\lambda = 19°$ and latitude $\beta = 25°$.

Bibliography

[B08] Beuzit, J.-L., Feldt, M., Dohlen, K., et al. 2008, in Proceedings of SPIE, Vol. 7014, Ground-based and Airborne Instrumentation for Astronomy II, 701418

[F03] Fusco, T., Mugnier, L. M., Conan, J.-M., et al. 2003, in Proceedings of SPIE, Vol. 4839, Adaptive Optical System Technologies II, ed. P. L. Wizinowich & D. Bonaccini, 1065–1075

[O10] Ostro, S. J., Magri, C., Benner, L. A. M., et al. 2010, Icarus, 207, 285

[S17] Schmid, H. M., Bazzon, A., Milli, J., et al. 2017, Astronomy and Astrophysics, 602, A53

[V15] Viikinkoski, M., Kaasalainen, M., & Ďurech, J. 2015, Astronomy and Astrophysics, 576, A8

[V16] Viikinkoski, M. 2016, PhD thesis, Tampere University of Technology

[V18] Vernazza et al., The impact crater at the origin of the ∼100 Myrs old Julia family detected via VLT/SPHERE observations?, submitted to A&A

EPSC Abstracts
Vol. 12, EPSC2018-178, 2018
European Planetary Science Congress 2018

Physical properties of asteroids using the WFCAM Transit Survey and the Virtual Observatory

M. Cortés-Contreras (1,2), F. M. Jiménez-Esteban (1,2,3), E. Solano (1,2), B. Carry (4) and C. Rodrigo (1,2)
(1) Departmento de Astrofísica, Centro de Astrobiología (CSIC-INTA), ESAC Campus, Camino Bajo del Castillo s/n mcortes@cab.inta-csic.es) , (2) Spanish Virtual Observatory, Spain, (3) Suffolk University, Madrid Campus, C/ de la Viña 3, 28003, Madrid, Spain, (4) Université Côte d'Azur, Observatoire de la Côte d'Azur, CNRS, Lagrange, 06304, Nice, France

Abstract

We describe here a methodology to identify asteroids serendipitously observed in large-area astronomical surveys using Virtual Observatory tools such as SkyBoT, TOPCAT, and STILTS. The application of this method on the WFCAM Transit Survey is demonstrated.

We provide almost 15,000 accurate positions (mean RMS 0.15 arcsec) and J-band magnitudes (typical accuracy of 0.11 mag) for over 1600 asteroids. From the repeated observations we build light curves and use them to determine the asteroid fundamental physical parameters, such as their rotational period or their multiplicity.

1. Introduction

Most of the $\sim$750,000 solar system small bodies known today are asteroids. Their study is motivated by their intrinsic importance as remnants of the early stages of the solar system formation and by practical reasons concerning space exploration and their frequent impacts with the Earth.

Wide imaging surveys, in particular those located not far from the ecliptic, offer the opportunity to discover and characterize asteroids serendipitously observed (e.g. [6]). Among them, exoplanets surveys are excellent resources to get dense lightcurves of asteroids as both types of targets share similar observing requirements: large field of views (FOV), long sequences, and short cadence. Lightcurves can be then used to determine fundamental physical parameters of asteroids. Indeed, the asteroid's shape, rotational period and the scattering properties of the surface can be determined from the analysis of the changes on the asteroid's brightness due to changes in its geometry.

In this study we have made use of the WFCAM Transit Survey (WTS), with 200 nights over five years at the 3.8-m United Kingdom Infrared Telescope (UKIRT). The purpose of WTS was to perform the first ever systematic near-infrared search for transiting exo-planets around cool dwarfs. It ran as a backup programme when observing conditions were not good enough. As a consequence, the observations were not uniformly distributed over time. WTS targeted four fields, each 1.6 square degrees in size, in J-band and observed them once in the $ZYHK_s$ filters. The four detectors of WFCAM cover 13.65 arcmin $\times$ 13.65 arcmin each and have a plate scale of 0.4 arcsec.

2 Methodology

Our workflow makes use of SExtractor ([1]), Aladin Sky Atlas ([3] and [2]), the STILTS package ([7], as well as the IDL and Python programming languages.

2.1 Pre-processing and source extraction

We gathered 30 877 bias and flat corrected and astrometrically calibrated WTS images from the WFCAM Science Archive[1]. We helped us with Aladin to extract the subimage taken by each of the four detectors and manage them independently. After discarding images observed in other filters than J and defective images, we searched for asteroids in 121 462 subimages, all in the J band.

Sources were detected by running SExtractor on every subimage. Using the Gaia DR1 ([4] and [5]) catalogue as a reference we estimated an average astrometric error for the SExtractor sources of 0.15 arcsec ($\sigma_{SExtractor}$).

To distinguish between moving asteroids and any other source in the field, we built a catalog composed by all SExtractor sources detected at the same position

[1] http://wsa.roe.ac.uk/

in different images within an error of 0.4 arcsec. This catalog covers the four regions observed in the WTS and contains 1 049 284 unique sources, mainly celestial sources but also bad pixels and artifacts. From now on, we will refer to this catalogue as the *Non-moving Source Catalog*.

2.2 Asteroid identification

We identified the asteroids lying in our images at the epoch of observation making use of the Virtual Observatory-compliant service SkyBoT (Sky Body Tracker, Berthier et al. 2006). SkyBoT provides a fast and simple cone-search method to list all known asteroids within a given FOV at a given epoch.

For each subimage, we obtained the list of asteroid counterpart candidates by cross-matching the SExtractor catalog with the SkyBoT positions of the asteroids lying in the image within a 3σ radius, where σ is given by:

$$\sigma = sqrt({\sigma_{SExtractor}}^2 + {\sigma_{SkyBoT}}^2), \qquad (1)$$

According to Skybot, there were 41 804 asteroid positions lying inside the field of view of the images in the J-band. For 14 685 of them, we obtained one asteroid counterpart candidate per asteroid position after removing the false counterparts using the *Non-moving Source Catalog* and applying five additional quality control tests:

- Nearly constant separations between the SExtractor position and the one provided by SkyBot.
- For each night, less than 20% difference in right ascention and declination proper motions between those computed from SExtractor counterparts and those provided by SkyBoT. If true, we flagged them with *A* and with *B* otherwise.
- Linear regression test within the same night. If $|r| \geq 0.9$ we assumed linearity and flagged them with *A* flag and with *B* otherwise.
- $(V - J)$ colors between 0.6 mag and 2.3 mag are flagged with *A*, assuming $(V - J)$ = 1.2–1.7 for asteroids and a maximum light curve amplitude of 0.6 mag. *B* flag otherwise.

Almost 98% of the remaining 25589 positions of asteroids for which we do not have candidate counterparts correspond either to asteroids with magnitudes close or beyond the magnitude limit of the images or asteroids that are being obscured by a bright field star.

Table 1: Number of asteroids and detections.

Class	# asteroids (fraction)	# asteroid detections
Main Belt	1492 (93.0)	13608
Hungaria	53 (3.3)	370
Trojan	42 (2.6)	490
Mars-Crosser	26 (1.6)	196
Near-Earth Asteroid	7 (0.4)	21

2.3 Asteroid characterization

The 14 685 confirmed asteroid positions correspond to 1 620 asteroids, for which we provide α and δ coordinates, $\mu_\alpha \cos(\delta)$ and μ_δ proper motions, epoch, J band magnitude and test flags. The number of asteroid and asteroid detections in the survey is summarized in Table 1 for each class of object.

Light curve building requires the comparison of asteroid magnitudes obtained at different nights. The photometric calibration of each subimage was done using the 2MASS catalogue. The distribution of magnitudes of the **14 585** asteroid counterparts identified in this work peaks at around 18.3 mag, which reflects the limiting magnitude of the survey although asteroids up to 20.6 mag have been detected.

The analysis of the light curves and the determination of the associated physical parameters is currently on-going.

3. Summary and Conclusions

We have developed a robust methodology to identify asteroids in large area surveys using Virtual Observatory tools. We proved this method to be efficient making use of the WFCAM Transit Survey. We were able to identify over 1 600 asteroids in near 15 000 different epochs for which we provide positions, proper motions and J band magnitudes, as well as physical parameters for a subset of them. Asteroid positions have been reported to the Minor Planet Center[2] to improve their associated orbital parameters.

[2]http://minorplanetcenter.net

Acknowledgements

This research has made use of the Spanish Virtual Observatory (http://svo.cab.inta-csic.es) supported from the Spanish MINECO/FEDER through grants AyA2011-24052 and AyA2014-55216.

References

[1] Bertin, E. & Arnouts, S., 1996, A&AS, 117, 393

[2] Boch, T. & Fernique, P., 2014, ASPC, 485, 277

[3] Bonnarel, F., Fernique, P., Bienaymé, O.; Egret, D. Genova, F., Louys, M., Ochsenbein, F., Wenger, M., Bartlett, J. G., 2000, A&AS, 143, 33

[4] Gaia Collaboration, A. G. A. Brown, A. Vallenari, T. Prusti, J. H. J. de Bruijne, F. Mignard, R. Drimmel, C. Babusiaux, C. A. L. Bailer-Jones, U. Bastian and et al., 2016a, A&A, 595, A2

[5] Gaia Collaboration, T. Prusti, J. H. J. de Bruijne, A. G. A. Brown, A. Vallenari, C. Babusiaux, C. A. L. Bailer-Jones, U. Bastian, M. Biermann, D. W. Evans and et al., 2016b, A&A 595, A1

[6] Popescu, M. and Licandro, J. and Morate, D. and de León, J. and Nedelcu, D. A. and Rebolo, R. and McMahon, R. G. and Gonzalez-Solares, E. and Irwin, M. 2016, A&A, 591, A115

[7] Talor, M.B. 2005, ASPC, 347, 29

EPSC Abstracts
Vol. 12, EPSC2018-489, 2018
European Planetary Science Congress 2018

Thermal properties of slowly rotating asteroids

Anna Marciniak (1), Thomas Müller (2), Víctor Alí-Lagoa (2) and Przemysław Bartczak (1)
(1) Astronomical Observatory Institute, Faculty of Physics, A. Mickiewicz University, Słoneczna 36, 60-286 Poznań, Poland, (am@amu.edu.pl) (2) Max-Planck-Institut für extraterrestrische Physik, Giessenbachstrasse 1, 85748 Garching, Germany

Abstract

Thermal properties of asteroids: thermal inertia, size, albedo, and surface roughnes require physical properties like spin axis position, rotation period and shape to be known before they can be determined. We focus on slowly rotating main belt asteroids to decrease selection effects in their spin and shape properties, but also in thermal inertia values, which are largely missing for slow rotators. Using multi-mission infrared data we apply our models from lightcurve inversion in the thermophysical modelling process. As a result we obtain scaled shape models with thermal properties determined. We find both large and small values of thermal inertia, what indicates distinct properties of surface regolith.

1. Selection effects

1.1. Spins and shapes

Slowly rotating asteroids (P > 12 hours) are challenging in spin and shape modelling, requiring large amounts of observing time in order to register their full optical lightcurves, especially when slow rotation is coupled with small amplitude of brightness variations. As a result the sample of spin and shape modelled asteroids is now dominated by short-period and large-amplitude targets - those with elongated shapes and extreme values of spin axis obliquity [9].

This bias might influence studies of e.g. evolution of asteroids under Yarkovski and YORP effects [12], [5], or the outcomes of impacting events [11].

1.2. Thermal properties

This selection effect also propagates to studies of asteroid thermal properties, which cannot be reliably determined without precise spin and shape models. Our recent study has shown that combining data from a network of ground based observatories with data from infrared space telescopes (mainly from IRAS, AKARI, and WISE) has a huge potential in asteroid physical studies, providing detailed shape models with absolute size scales, albedos and thermal inertia values [10]. Such thermophysical models have been obtained for around 200 of asteroids so far, and among them only a small fraction rotate slowly [2], [6].

It has not been much investigated yet if thermal inertia of very slow rotators can ever be determined. Relatively small distance between sub-solar point and the warmest, afternoon part of the asteroid surface might challenge such determinations. On the other hand, if it can (and we found that true in most studied cases), then it should contain information on the material properties of deeper, sub-regolith layers of the surface [7]. This way the density and thermal conductivity of such layers, and also regolith grain size and packaging tied to the surface roughness can be studied [4].

2. Results

Our photometric observing campaign resulted in a substantial number of spin and shape models of slowly rotating asteroids based on dense lightcurves. To create the models we used convex inversion method [8] and in some cases also non-convex SAGE algorithm [1]. We then applied thermophysical models (e.g.[2]) to determine their sizes and albedos, with thermal inertia and indication of the level of surface roughness. It is worth noting that internally consistent good fits were simultaneously obtained for data from a few different infrared space observatories, giving more confidence to our results. One example is shown in Fig. 1

In a few cases a mirror pole symmetry was broken, as one of two solutions for the pole gave clearly better fit to thermal data. Found thermal inertia values are often large (up to 125 SI units), as expected. Sizes of main belt targets in our sample range from 20 to 130 km. So far mostly relatively large Γ values have been observed in this size range [2].

However in some cases Γ values that we found are surprisingly small (around 10 SI units), indicating a fine, mature regolith on their surfaces. Alternatively,

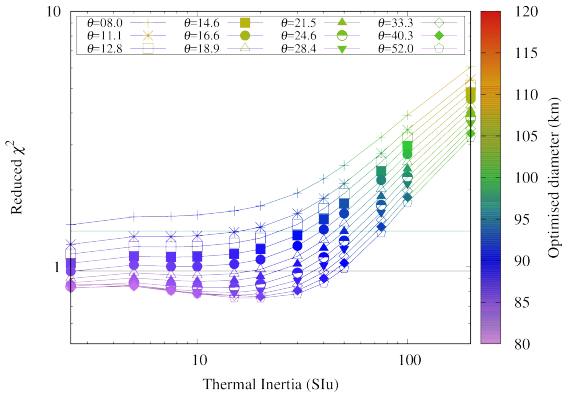

Figure 1: χ_2 plots versus thermal inertia values for asteroid 195 Eurykleia (P=16.52179 h). The different surface roughness levels are shown with different point types, and the best-fitting diameter for each model is coded in the colour palette. The horizontal lines mark the 1-sigma (lower) and 3-sigma (upper) limits below which models can be considered to fit the data acceptably.

small thermal inertia might be an indicator of colder temperatures of deeper subsurface layers, to which a heat wave can penetrate in case of long-period targets, provided the density does not change with depth [3].

3. Summary and Conclusions

By studying slow rotators we are filling the gaps in a few areas of asteroid physics. We debias the set of known spin and shape parameters, providing precise models based on dense lightcurves for targets that cannot be studied otherwise (e.g. where available sparse data from large surveys are often insufficient). This way we also provide largely missing type of targets for thermophysical modelling, and find a wide range of thermal inertias, indicating large differences of the regolith type on the surface or in subsurface material properties. In the near future we are going to verify various hypotheses concerning thermal inertia dependence on the rotation period, by studying more targets with periods longer than 20 hours.

Acknowledgements

This work was supported by grant no. 2014/13/D/ST9/01818 from the National Science Centre, Poland. The research leading to these results has received funding from the European Union's Horizon 2020 Research and Innovation Programme, under Grant Agreement no 687378.

References

[1] Bartczak, P., Dudziński G.: Shaping asteroid models using genetic evolution (SAGE), MNRAS, 473, pp. 5050-5065, 2018.

[2] Delbo, M., Mueller, M., Emery, J. P et al.: Asteroid Thermophysical Modeling, in: Asteroids IV, Tucson: University of Arizona Press, pp. 107-128, 2015.

[3] Ďurech, J., Delbo, M., Carry B., et al.: Asteroid shapes and thermal properties from combined optical and mid-infrared photometry inversion Astronomy Astrophys., 604, A27, 2018.

[4] Gundlach, B., and Blum, J.: A new method to determine the grain size of planetary regolith, Icarus, 223, pp. 479 - 492, 2013.

[5] Hanuš, J., Ďurech, J., Brož M. et al.: Asteroids' physical models from combined dense and sparse photometry and scaling of the YORP effect by the observed obliquity distribution, Astronomy Astrophys., 551, A67, 2013.

[6] Hanuš, J., Delbo, M., Ďurech, J. et al.: Thermophysical modelling of main-belt asteroids from WISE thermal data, Icarus, 309, pp. 297-337, 2018.

[7] Harris, A. W., and Drube, L.: Thermal Tomography of Asteroid Surface Structure, Astrophys. J., 832, p. 127, 2016.

[8] Kaasalainen, M., Torppa, J., Muinonen, K.: Optimization Methods for Asteroid Lightcurve Inversion. II. The Complete Inverse Problem, Icarus, 153, pp. 37-51, 2001.

[9] Marciniak, A., Pilcher, F., Oszkiewicz, D. et al.: Against the biases in spins and shapes of asteroids, Planet. Space Sci., 118, pp. 256-266, 2015.

[10] Marciniak, A., Bartczak, P., Müller, T., et al.: Photometric survey, modelling, and scaling of long-period and low-amplitude asteroids, Astronomy Astrophys., 610, A7, 2018.

[11] Takeda, T. and Ohtsuki, K.: Mass dispersal and angular momentum transfer during collisions between rubble-pile asteroids. II. Effects of initial rotation and spin-down through disruptive collisions., Icarus, 202, pp. 514-524, 2009.

[12] Vokrouhlický, D., Bottke, W. F., Chesley, S. R. et al.: The Yarkovsky and YORP Effects, in: Asteroids IV, Tucson: University of Arizona Press, pp. 509-531, 2015.

EPSC Abstracts
Vol. 12, EPSC2018-534-1, 2018
European Planetary Science Congress 2018

ESO/VLT/SPHERE Survey of D>100km Asteroids (2017-2019): (16) Psyche

M.Viikinkoski (1) P. Vernazza (5), M. Marsset (2), J. Hanuš (3), B. Carry (4), A. Drouard (5), R. Fetick (5), F. Marchis (6), E. Podlewska (7), P. Bartczak (7), T. Santana-Ros (7), M. Birlan (8), C. Dumas (9), M. Kaasalainen (1), B. Yang (10), J. Ďurech (3), L. Jorda (5), P. Lamy (5), A. Vigan (5), T. Fusco (5), T. Michalowski (7), A. Marciniak (7), M. Pajuelo (8), P. Michel (4), P. Tanga (4), J. Berthier (8), F. Vachier (8), J. Castillo-Rogez (11), O. Witasse (12), F.Cipriani (12), E. Jehin (13), M. Ferrais (13) (1) Tampere University of Technology, Mathematics Laboratory, Finland (matti.viikinkoski@tut.fi) (2) Queen's University of Belfast, UK (3) Charles University in Prague, CZ (4) OCA, France (5) Laboratoire d'Astrophysique de Marseille, France (6) Seti institute, USA (7) Astronomical Observatory Institute, Faculty of Physics, Adam Mickiewicz University, PL (8) IMCCE, FR, (9) TMT, USA, (10) ESO, CL, (11) JPL, USA, (12) ESTEC, NL, (13) Institut d'Astrophysique de l'Université de Liège , BE

Abstract

Asteroid (16) Psyche is the largest of the M-type asteroids in the main belt. High radar albedo is an indicative of metallic nickel-iron composition and albedo variegation both at radar and visible wavelengths suggest surface heterogeneity. Recent studies [1, 2] estimate that Psyche is an exposed core (either intact or a rubble pile) of a Vesta-like planetesimal. The uniqueness of Psyche is the main reason for its selection as the target of Discovery-class mission, which is planned to be launched in 2022.

The asteroid has been previously observed with both the Arecibo range-Doppler radar and the Keck adaptive optics system. While the Keck observations covered most of the asteroid's surface, their resolution were insufficient to distinguish any details. The range-Doppler images, on the other hand, showed a detailed view of the southern hemisphere, although everything above 45° latitude was unseen by the radar.

We present new high-resolution images obtained with the SPHERE/ZIMPOL visible light adaptive optics camera at VLT during May-June 2018. The adaptive optics system facilitates observing at the resolution close to the diffraction limit, which is approximately 18 mas in the visible band. The camera pixel size is 3.6 mas, or about 6 km projected at the distance of Psyche. Observed at opposition, the images provide a highly detailed view of the previously unobserved northern hemisphere.

We use the SPHERE adaptive optics images, together with the earlier Keck data, stellar occultations, lightcurves, and range-Doppler images to derive a non-convex 3-D shape model of the asteroid. We estimate shape and size uncertainties, analyze prominent topographic features and study their consistency across observations.

References

[1] Shepard, M. K. and Richardson, J. and Taylor, P. A. and Rodriguez-Ford, L. A. and Conrad, A. and de Pater, I. and Adamkovics, M. and de Kleer, K. and Males, J. R. and Morzinski, K. M. and Close, L. M. and Kaasalainen, M. and Viikinkoski, M. and Timerson, B. and Reddy, V. and Magri, C. and Nolan, M. C. and Howell, E. S. and Benner, L. A. M. and Giorgini, J. D. and Warner, B. D. and Harris, A. W.: Radar observations and shape model of asteroid 16 Psyche, Icarus, vol. 281, 2017.

[2] Jack D. Drummond, William J. Merline, Benoit Carry, Al Conrad, Vishnu Reddy, Peter Tamblyn, Clark R. Chapman, Brian L. Enke, Imke de Pater, Katherine de Kleer, Julian Christou, Christophe Dumas: The triaxial ellipsoid size, density, and rotational pole of asteroid (16) Psyche from Keck and Gemini AO observations 2004–2015, Icarus, vol 305, 2018.

EPSC Abstracts
Vol. 12, EPSC2018-746, 2018
European Planetary Science Congress 2018

The Thermal Response of Asteroid Surfaces: Results from ESO Large Programme

S. C. Lowry (1), A. Rozek (1), B. Rozitis (2), T. Zegmott (1), S. F. Green (2), C. Snodgrass (2), A. Fitzsimmons (3), P. Weissman (4), and E. C. Brown (5).
(1) University of Kent, UK (s.c.lowry@kent.ac.uk), (2) The Open University, UK, (3) Queens University Belfast, UK, (4) Planetary Science Institute, USA, (5) University of Oxford, UK.

Abstract

The (YORP) effect [1] is a torque due to incident solar radiation and the subsequent recoil effect from the anisotropic emission of thermal photons on small bodies in the Solar System. The YORP effect can: change rotation rates and spin-axis orientations over relatively short time-scales; modify orbits (semi-major axis drift from the related Yarkovsky effect depends on the obliquity) and thus plays a key role in replenishment of the near-Earth asteroid (NEA) population; cause regolith mobility and resurfacing as spin rates increase, form binary asteroids through equatorial mass loss and re-aggregation and cause catastrophic disruption. When we began our systematic monitoring programme in 2010, the YORP effect had only been detected for three asteroids [2-4] with a marginal detection following in 2012 [5]. That has now increased to six [6-7]. All detections so far are in the spin-up sense, and theoretical studies are making progress in explaining this observation [8]. However, a much larger statistical sample is required to robustly test this theory. We are conducting an observational programme of a sample of NEAs to detect YORP-induced rotational accelerations. For this we use optical photometry from a range of small to medium size telescopes. This is supplemented by thermal-IR observations and thermophysical modelling to ascertain expected YORP strengths for comparison with observations. For selected objects, we use radar data to determine shape models. We will present our latest results from this programme.

1. Observational Campaign:

Optical photometry and the detection of YORP: Detection of rotational acceleration requires measurement of phase shifts in rotational lightcurves at a minimum of three apparitions. Our observational programme focuses on ~km-sized NEAs with short spin periods to allow suitable lightcurves to be obtained at multiple apparitions with short runs on a range of moderate-sized telescopes. We have acquired a considerable dataset on our target NEAs, mainly through our ESO 3.6m NTT Large Programme (185.C-1033), but also supporting observations from the 2.5m Isaac Newton Telescope and the 2m Liverpool Telescope (La Palma, Spain), and the 5m Hale Telescope at Palomar Observatory (USA), among many others. Lightcurve data from the programme will also be linked to previous published data where available. We use an established light curve inversion code, e.g. [9], modified to include YORP-induced sidereal rotation period changes, to derive shape and spin state models and identify the YORP effect (See Fig. 1).

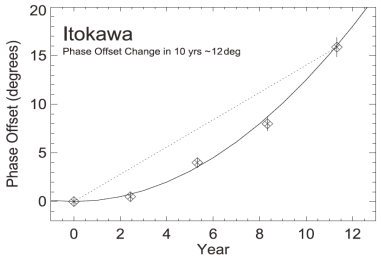

Figure 1. Rotational-phase changes (φ) in Itokawa observed from 2001-2013 [6]. The strong quadratic variation of φ is consistent with YORP-induced rotational acceleration. This is the characteristic signature of YORP that we are searching for with our NEA targets and modelling methods.

Thermal-IR observations and thermophysical modelling: Mid-IR observations provide valuable constraints on size, albedo and surface roughness, required to model the YORP effect, as well as thermophysical properties. We have a parallel programme to obtain mid-IR photometry for all targets that are sufficiently bright for detection with the VISIR instrument on ESO's 8.2m VLT (185.C-1034, 190.C-0357, 197.C-0816) as well as a

Spitzer/IRAC programme (#11097), augmented by archival data from WISE [10]. YORP effect predictions are made using the Advanced Thermophysical model (ATPM), e.g. [11], with shape models from our lightcurve analysis or derived from radar data (see Fig. 2).

Planetary radar programme: For selected objects, we have radar data available. Radar observations can greatly improve the spin-state analysis by providing a fully independent shape model, thus greatly reducing the range of potential solutions for YORP. The ability of radar to detect surface concavities is an important advantage as many asteroids are reported to have bi-lobed or contact-binary configurations [12]. Radar data can also be merged with optical lightcurve data to provide tighter constraints on rotational pole positions and shape and spin-states. Such detailed shape models also allow for more rigorous modelling of the YORP and Yarkovsky effects [13]. The radar observations used in this programme were obtained using the Arecibo Planetary Radar (Puerto Rico, PID: R2959, R3036) and Goldstone (USA) facilities.

2. Latest Results

We have already detected YORP and inferred density heterogeneity in (25143) Itokawa (Fig. 1) [6]. We will present our latest results and progress on YORP detections/upper limits for a subset of NEAs from our programme, which include: (1917) Cuyo (Fig. 2), (8567) 1996 HW1, (85990) 1999 JV6, 6053, and 1950 DA. Our analysis of observations also yields several additional important results in relation to the physical properties of several of these NEAs. For example, the shape of Cuyo resembles the oblate spheroid or 'spinning top' shape first observed on NEA 1999 KW4 [14]. This shape is due in part to radiative torques. While we do not see a strong YORP signature in the data, this asteroid has likely experienced YORP-induced shape modifications. Furthermore, thermophysical analysis, utilizing our thermal observations and the shape model, reveal that material near the equatorial ridge may be leaving the surface (See Fig. 2). Cuyo has a low thermal inertia of 24 J m^{-2} K^{-1} $s^{-1/2}$, indicating a surface significantly reduced in surface boulders. Our analysis of combined radar and optical photometry of 1999 JV6 reveal a distinctive bi-furcated shape, similar to 1996 HW1 [15] and Itokawa [16]. This asteroid is likely to be the result of a collapsed binary system. We also detect a transverse non-gravitational acceleration (NGA) of (-1.6 ± 0.2) × 10^{-12} m s^{-2} in the orbital motion of this object, based on our radar astrometry. Thermophysical analysis of Spitzer data, combined with the shape model can attribute this NGA detection to the Yarkovsky effect, and also yields a low bulk density measurement of ≤ 830 g cm^{-3}. Asteroid 1999 JV6 may therefore be of cometary origin. These results will be discussed in detail at the meeting, along with the full range of latest results from this on-going programme.

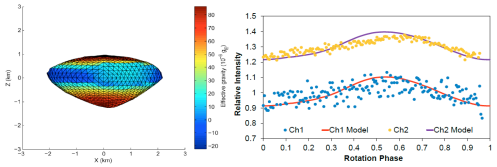

Figure 2. (1917) Cuyo shape model indicating negative effective gravity near the equator (left), used to fit Spitzer/IRAC light-curves (right).

Acknowledgements

We thank all the staff at the observatories involved in this study for their support. SCL, AR, and SFG acknowledge support from the UK Science and Technology Facilities Council and the Southeast Physics Network (SEPnet). BR acknowledges support from the Royal Astronomical Society in the form of a research fellowship.

References

[1] Rubincam (2000). *Icarus 148,* 2. [2] Lowry et al. (2007). *Science 316*, 272. [3] Kaasalainen et al. (2007). *Nature 446*, 420. [4] Durech et al. (2008). *A&A 489,* L25. [5] Durech et al (2012). *A&A 547*, A10. [6] Lowry et al. (2014). *A&A 562*, A48. [7] Durech et al. (2018), *A&A* 609, A86. [8] Golubov, et al. (2014). *ApJ* 794, 22. [9] Mainzer et al. (2011). ApJ 743, 156. [10] Kaasalainen et al. (2003). *A&A 405*, L29. [11] Rozitis & Green (2012). *MNRAS 423*, 367. [12] Benner et al. (2015). In *Asteroids IV*, 165–182. [13] Rozitis & Green (2013). *MNRAS* 433, 603. [14] Ostro et al. (2006). *Science* 314, 1276.
[15] Magri et al. (2011). *Icarus* 214, 210. [16] Demura et al. (2006). *Science* 312, 1347.

EPSC Abstracts
Vol. 12, EPSC2018-747, 2018
European Planetary Science Congress 2018

Determination of spin axes and shapes of NEAs from one apparition

Tomasz Kwiatkowski
Astronomical Observatory, Faculty of Physics, Adam Mickiewicz University, Poznań, Poland
(tkastr@vesta.amu.edu.pl).

1. Abstract

The majority of asteroid models, which include the rotation period, spin axis and shape, are derived from the analysis of asteroid light variations, observed at different geometries. While for the Main Belt asteroids it takes at least three, well spaced oppositions to collect the necessary data, some near-Earth asteroids, when passing by the Earth, sweep long arcs in the sky enabling observations at different geometries. This potentially can help in determination of their models from relatively short observing campaigns.

It can be argued that the minimum arc length in the sky, covered by photometric observations, needed to derive a uniqe spin axis and shape model for a NEA in favourable conditions is about 120 deg (Josef Durech, private communication). Hence it is interesting to check how often NEAs are observable in such a way that a coordinated, world-wide photometric campaign can collect enough data for derivation of their models from a short, one to two months observing period. Apart from the length of arc in the sky, other observing conditions should be taken into account such as the Moon conditions, background stars' density, asteroid brightness, sky movement, etc.

To answer those questions computations of NEA ephemerides have been performed using both the historic orbits of the NEAs discovered in the past as well as the simulated orbits based on the Granvik et al. model of the NEO population [1]. They were then used to select objects which can potentially be used for spin axis and shape analysis. The analysis of the obtained results will be presented at the conference.

2. References

[1] GRANVIK, M., MORBIDELLI, A., JEDICKE, R., BOTTKE, W. F., BOLIN, B., BESHORE, E., VOKROUHLICKY, D., NESVORNY, D., MICHEL, P. (2013) A New Population Model of the Orbits and Absolute Magnitudes of Near-Earth Objects. AAS/Division for Planetary Sciences Meeting Abstracts #45, 106.02

EPSC Abstracts
Vol. 12, EPSC2018-832, 2018
European Planetary Science Congress 2018

EPSC
European Planetary Science Congress

Physical parameters of near-Earth asteroid 2017 VR12 from radar and optical photometric observations

Yu. S. Bondarenko (1), D. A. Marshalov (1), Yu. D. Medvedev (1), G. I. Kornienko (2), A. V. Kochergin (2), M. S. Zheltobryukhov (2) and L. A. Benner (3)
(1) Institute of Applied Astronomy of the Russian Academy of Sciences, Russia (bondarenko@iaaras.ru), (2) Ussuriysk Astrophysical Observatory of the Far Eastern Branch of the Russian Academy of Sciences, Russia, (3) Jet Propulsion Laboratory, California Institute of Technology, USA

Abstract

We report results of bistatic radar and optical photometric observations of near-Earth Asteroid 2017 VR12. This asteroid closest approach was on March 7 at a distance of 0.0097 au. The continuous wave echo power spectra were obtained during March 5, 2018 using Goldstone radar to transmit and 32-m radio telescopes in Zelenchukskaya and Badary observatories to receive the echoes. Light curve data were made using 0.65 m telescope at the Ussuriysk Astrophysical Observatory on March 6, 2018. We find that the asteroid rotates with a period 1.378 $\pm$ 0.03 hours and have a pole-on silhouette breadth of 138 m. Our estimates of radar albedo are 0.32 $\pm$ 0.04 and 0.31 $\pm$ 0.04 and the circular polarization ratios are 0.36 $\pm$ 0.02 and 0.34 $\pm$ 0.01 for Zelenchukskaya and Badary correspondingly.

1. Introduction

Asteroid 2017 VR12 was discovered on November 10, 2017 by the 60-inch Pan-STARRS 1 telescope at Haleakala Observatory. 2017 VR12 is an Amor class near-Earth asteroid (NEA) with an orbital semi-major axis of 1.3696 au and a perihelion distance of 1.0004 au and is classified as a "Potentially Hazardous Asteroids" by the Minor Planet Center. On March 7, 2018 this asteroid approached the Earth within 0.0097 au which was the closest encounter since its discovery. Pravec et al. (http://www.asu.cas.cz/ ppravec) reported a light curve period of 1.37752 $\pm$ 0.00007 h with an amplitude of 0.2. However, the physical parameters of this asteroid were unknown except its absolute magnitude of 20.6 which, for mean optical albedo from 0.05 to 0.5 suggests a diameter from 450 to 140 meters.

In March 2018, we had the opportunity to conduct a bistatic radar observations of 2017 VR12 in cooperation with the Goldstone planetary radar and also obtain photometric observations from Ussuriysk Astrophysical Observatory. Here we present a physical parameters of 2017 VR12 derived from radar and light curve data.

2. Photometric observations

We observed 2017 VR12 at the Ussuriysk Astrophysical Observatory on March 6, 2018 with the 0.65 m telescope equipped with a KAF-4301E CCD. The observations began at 11:50:39 UT and covered 2.57 h during which 500 images of the asteroid were taken through a clear filter with an interval between frames and exposure time of 10 seconds and resolution of 3.8 arc seconds per pixel. The asteroid's magnitude was measured relative to 16 comparison stars from the UCAC4 catalog. Fig. 1 shows the light curve of the asteroid 2017 VR12 obtained as a result of observations. The average brightness of the asteroid was 11.8 magnitude and varied within 0.6 magnitude. One can see periodic variations in brightness including two maxima and two minima of different amplitudes, which can occur due to the precession of the rotation axis. Using a Fourier series method to the light curve data we obtained the most probable rotation period of 1.378 $\pm$ 0.03 h.

3. Radar observations

We observed 2017 VR12 on March 5, 2018 using 32-m radio telescopes in Zelenchukskaya and Badary observatories. Goldstone radar transmitted 150 kW circular polarized continuous wave (CW) signal at 8560 MHz (3.5 cm). Echoes were recorded simultaneously in the same (SC) and opposite (OC) senses of circular polarizations as the transmission. Taking into account the Doppler frequency as a function of time we applied the Fourier transform to the echo time se-

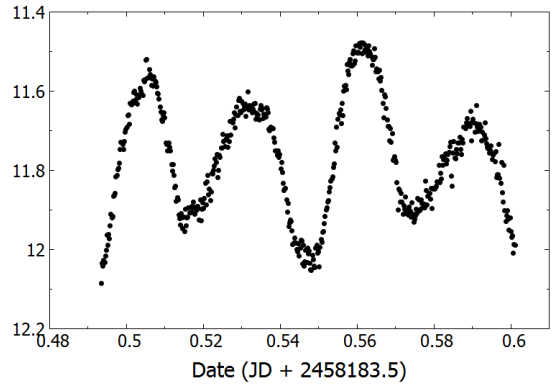

Figure 1: Lightcurve data of 2017 VR12 obtained at Ussuriysk Astrophysical Observatory on March 6, 2018.

ries. As a result we obtained CW echo power spectra for 9 minutes integration time with 1 Hz frequency resolution. At the Fig. 2 you may see the OC and SC continuous wave echo power spectra of 2017 VR12 obtained at Zelenchukskaya (A) and Badary (B) observatories. Echo power is plotted in standard deviations versus Doppler frequency relative to the estimated frequency of echoes from the asteroid's center of mass.

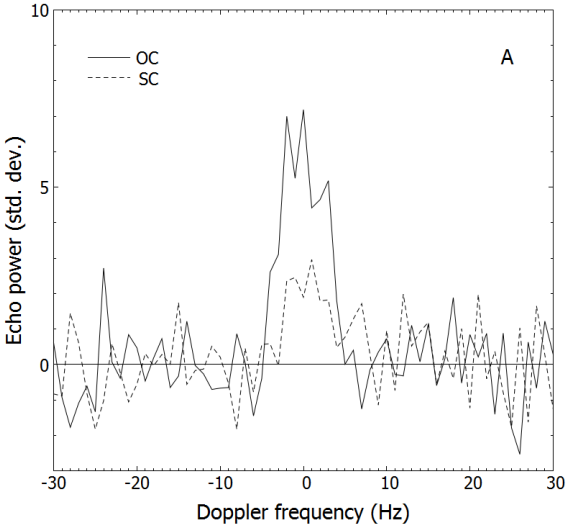

Knowing the rotation period and instantaneous echo power spectra bandwidth $\sim$10 Hz and assuming zero angle between the observer line-of-sight and the object's apparent equator we may estimate the lower bound on the asteroid's maximum pole-on breadth of

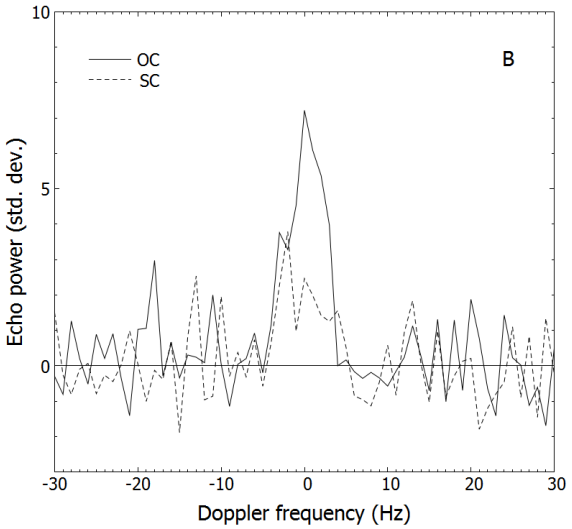

Figure 2: Continuous wave echo power spectra of 2017 VR12 obtained at Zelenchukskaya (A) and Badary (B) observatories on March 5, 2018 from 4:16 to 4:25 UT. Each curve has a frequency resolution of 1 Hz. Solid and dashed lines denote echo power in the OC and SC polarizations.

138 m at the rotation phase ϕ. By integrating the CW spectra we obtained the radar albedo of 0.32 $\pm$ 0.04 for Zelenchukskaya and 0.31 $\pm$ 0.04 for Badary suggests S or M-class NEA with a bright surface [1]. The ratio of the integrated SC and OC signal is a measure of near-surface wavelength-scale roughness. We estimated the circular polarization ratios of 0.36 $\pm$ 0.02 and 0.34 $\pm$ 0.01 for Zelenchukskaya and Badary correspondingly, indicates that the near-surface of 2017 VR12 at decimeter scales is morphologically rougher than those of most radar-detected NEA's [2].

This work was supported by the Russian Scientific Foundation grant No 16-12-00071.

References

[1] Margi, C. et.al.: A radar survey of main-belt asteroids: Arecibo observations of 55 objects during 1999–2003, Icarus, Vol. 186, pp. 126-151, 2007.

[2] Benner, L. et.al.: Near-Earth asteroid surface roughness depends on compositional class, Icarus, Vol. 198, pp. 294-304, 2008.

EPSC Abstracts
Vol. 12, EPSC2018-1053, 2018
European Planetary Science Congress 2018

Asteroid spin properties derived from thermal data

Thomas Müller (1), Víctor Alí-Lagoa (1), Josef Ďurech (2), Anna Marciniak (3), Róbert Szakáts (4), and the SBNAF team
(1) Max-Planck-Institut für extraterrestrische Physik, Giessenbachstrasse 1, 85748 Garching, Germany (tmueller@mpe.mpg.de), (2) Astronomical Institute, Faculty of Mathematics and Physics, Charles University, V Holešovičḱach 2, 180 00, Praha 8, Czech Republic (3) Astronomical Observatory Institute, Faculty of Physics, A. Mickiewicz University, Słoneczna 36, 60-286 Poznań, Poland (4) Konkoly Observatory, Research Centre for Astronomy and Earth Sciences, Hungarian Academy of Sciences, H-1121 Budapest, Konkoly Thege Miklós út 15-17, Hungary

Abstract

Multiple optical lightcurves of asteroids are widely used to derive the object's shape and spin properties via standard lightcurve inversion methods. Thermal measurements are key ingredients for radiometric methods to derive size, albedo, and thermal properties of a given asteroid. However, thermal infrared data also contain crucial information about the object's spin properties. Depending on the amount of available thermal data and their quality, one can determine the object's sense of rotation or even constrain the spin-axis orientation. The thermal data also allow to verify shape solutions, and in some cases it is also possible to improve shape solutions. This is important for objects where the lightcurve inversion is ambiguous or fails completely. We present our methods and discuss possibilities and limitations of the new approach.

1. Introduction

Thermal infrared measurements typically comprise individual photometric points, sometimes multi-filter measurements (like from IRAS, AKARI or WISE), and only in very rare cases thermal ligthcurves coming from Spitzer or Herschel. These data are widely used to determine the size and albedo of small bodies via radiometric techniques. It is also possible to constrain the object's thermal properties and estimate surface roughness properties or even grain size distributions ([1] and references therein). However, in cases where thermal observations cover different aspect angles - preferentially also different phase angles and wavelengths - it is also possible to constrain the object's spin properties from thermal data alone (e.g., [8, 6]). A new method by Ďurech et al. [2] even allows to combine optical and thermal data to constrain multiple object properties simultaneously (see results on Ryugu by [11]). The combined approach is still difficult since it requires a careful weighting of data and a profund knowledge of the information content of a given (optical or thermal) data set. Here, we go one step back to look at the possibilities and limitations of radiometric techniques in the context of constraining the object's spin properties.

2. Applications

We use all available thermal data for a given object to find out if the object's spin properties can be identified. The combined data are analysed via a powerful thermophysical model code [3, 4, 5].

First, we look at a sample of large and well-known main-belt asteroids which only have a few thermal data points typically from the survey missions IRAS, AKARI, MSX and/or WISE, but only very few targeted thermal measurements from ground or space. For these poorly observed objects (at thermal wavelengths), our method allows to estimate at least the sense of rotation. We compare our results with the true spin properties as listed in the DAMIT database[1].

Other cases, like Bennu [8], Itokawa [10] and Ryugu [11], and also a few main-belt asteroid, have many more thermal data, covering different aspect angles, phase angles, and wavelengths. Here, the thermal data can put very strong constraints on the actual spin-axis orientation.

And even for Centaurs and trans-Neptunian objects it is often possible to distinguish between objects seen pole-on from objects seen equator-on. The thermal measurements in those cases are coming either from Herschel and/or Spitzer, for some near Centaurs also from WISE.

The comparison with "ground truth" - whenever available - shows the large scientific potential of thermal data in the context of asteroid spin properties. But

[1] http://astro.troja.mff.cuni.cz/projects/asteroids3D

it is important to understand the spin information content imprinted in thermal data before one can use them in a more general application where all available optical and thermal data are combined. For the full exploitation it is necessary to understand the wavelength, phase-angle and aspect-angle related effects, and to have a deeper understanding of the relative and absolute errors of a given measurement. We'll present our results and discuss the possiblities and limitations of the different approaches.

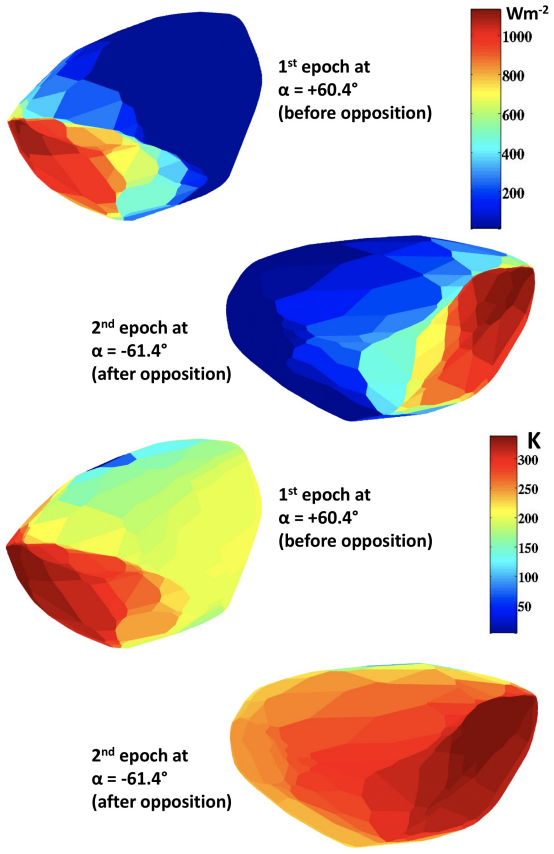

Figure 1: Top: The two figures show the insolation for the NEA 99942 Apophis before (left) and after (right) opposition, almost at exactly the same phase angles of around 61°. Bottom: The corresponding surface thermal pictures are very different, caused by the combined spin and thermal inertia properties. This example shows that thermal measurements contain information about the sense of rotation and in some cases can also constrain the spin-axis orientation. Figures adapted from [9].

Acknowledgements

The work was carried out in the context of the project "Small bodies: near and far" [12] which has received funding from the European Union's Horizon 2020 Research and Innovation Programme, under Grant Agreement no 687378.

References

[1] Delbo, M., Mueller, M., Emery, J. P. et al. 2015: Asteroid Thermophysical Modeling, Asteroids IV, P. Michel, F. E. DeMeo, and W. F. Bottke (eds.), University of Arizona Press, Tucson, p.107-128

[2] Ďurech, J., Delbo', M., Carry, B. et al. 2017: Asteroid shapes and thermal properties from combined optical and mid-infrared photometry inversion, A&A 604, 27D

[3] Lagerros, J. S. V. 1996: Thermal physics of asteroids. I. Effects of shape, heat conduction and beaming, A&A 310, 1011L

[4] Lagerros, J. S. V. 1997: Thermal physics of asteroids. III. Irregular shapes and albedo variegations, A&A 325, 1226L

[5] Lagerros, J. S. V. 1998: Thermal physics of asteroids. IV. Thermal infrared beaming, A&A 332, 1123L

[6] MacLennan, E. & Emery J. 2013: Constraints on Spin Axis and Thermal Properties of Asteroids in the WISE Catalog, DPS#45, id.208.19

[7] Marciniak, A., Bartczak, P., Müller, T. et al. 2017: Photometric survey, modelling, and scaling of long-period and low-amplitude asteroids, A&A 610, 7M

[8] Müller, T. G., O'Rourke, L., Barucci, A. M. et al. 2012: Physical properties of OSIRIS-REx target asteroid (101955) 1999 RQ36. Derived from Herschel, VLT/VISIR, and Spitzer observations, A&A 548, 36M

[9] Müller, T. G., Kiss, C., Scheirich, P. et al. 2014: Thermal infrared observations of asteroid (99942) Apophis with Herschel, A&A 556, 22M

[10] Müller, T. G., Hasegawa, S., Usui, F. 2014: (25143) Itokawa: The power of radiometric techniques for the interpretation of remote thermal observations in the light of the Hayabusa rendezvous results, PASJ 66, 52M

[11] Müller, T. G., Ďurech, J., Ishiguro, M. et al. 2017: Hayabusa-2 mission target asteroid 162173 Ryugu (1999 JU3): Searching for the object's spin-axis orientation, A&A 599, 103A

[12] Müller, T. G., Marciniak, A., Kiss, C. et al. 2018: Small Bodies Near and Far (SBNAF): a benchmark study on physical and thermal properties of small bodies in the Solar System, accepted for publication in Advances in Space Research

EPSC Abstracts
Vol. 12, EPSC2018-1107, 2018
European Planetary Science Congress 2018

Small Bodies Near and Far (SBNAF): Challenges in the Physical and Thermal Characterization of NEOs, MBAs and TNOs

T. G. Müller (1), A. Marciniak (2), C. Kiss (3), R. Duffard (4), V. Alí-Lagoa (1), P. Bartczak (2), M. Butkiewicz-Bąk (2), G. Dudziński (2), E. Fernández-Valenzuela (4), G. Marton (3), N. Morales (4), J. L. Ortiz (4), D. Oszkiewicz (2), T. Santana-Ros (2), P. Santos-Sanz (4), R. Szakáts (3), A. Takácsné Farkas (3), E. Varga-Verebélyi (3)
(1) Max Planck Institute for Extraterrestrial Physics, Garching, Germany; (2) Astronomical Observatory of A. Mickiewicz University, Faculty of Physics, Poznań, Poland; (3) Konkoly Observatory, Research Centre for Astronomy and Earth Sciences, Budapest, Hungary; (4) Instituto de Astrofísica de Andalucía - CSIC, Granada, Spain.

Abstract

We present results from the first two years of our EU Horizon2020-funded benchmark study (2016-2019) that addresses critical points in reconstructing physical and thermal properties of near-Earth, main-belt, and trans-Neptunian objects. The combination of the visual and thermal data from the ground and from astrophysics space missions (like Herschel, Spitzer, Kepler-K2 and AKARI) is key to improving the scientific understanding of these objects. The development of new tools will be crucial for the interpretation of much larger data sets, but also for the operations and scientific exploitation of interplanetary missions. We combine different methods and techniques to get full information on selected bodies: lightcurve inversion, stellar occultations, thermophysical modeling, radiometric methods, radar ranging and adaptive optics imaging. The applications to objects with ground-truth information from interplanetary missions Hayabusa, NEAR-Shoemaker, Rosetta, and DAWN allow us to advance the techniques beyond the current state-of-the-art and to assess the limitations of each method.

1. Targets

For our benchmark study on minor bodies we selected important targets which were already visited by spacecraft (or are currently visited), which have a wealth of data from different observing techniques available (or are candidates for being observed with new techniques), which are or will be useful in the calibration context, or which will allow us to address and solve specific scientific questions [1].

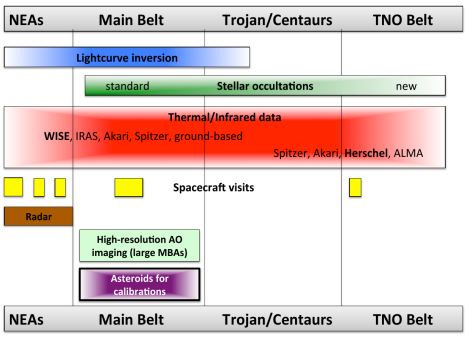

Figure 1: Overview of the SBNAF sample and the available observations.

2. Techniques

The characterization of small bodies is based on lightcurve inversion, radiometry, occultation, radar, and direct imaging techniques. We extract the crucial information from all available observations for a given target. The combination of different data sets leads to the development of new tools and methods which are validated against ground-truth information and to test capabilities and limitations. Figure 1 shows the different available techniques for our sample targets.

3. Tools, Services, and Products

ISAM (`http://isam.astro.amu.edu.pl/`) contains a collection of own and literature shape models for more than 900 asteroids. It allows to (i) display an asteroid orientation as seen from Earth at any date; (ii) to generate lightcurves; (iii) to animate the rota-

tion; (iv) to produce 3D views; (v) to investigate viewing and illumination geometries; and (vi) to download spin-shape solutions and generated products. The **Gaia-GOSA page** (`http://www.gaiagosa.eu`) is an interactive tool which supports observers in planning photometric observations of asteroids. The asteroid prediction tool is based on the Gaia orbit and scanning law (ESA) and SSO ephemerides (MPC). The planned **Asteroid IR database** will contain thermal IR/submm/mm observations of small bodies (NEAs, MBAs, Trojans, Centaurs, TNOs), including measurements from ground (MIR, submm, mm instruments), airborne (SOFIA), and space projects (IRAS, MSX, AKARI, ISO, Spitzer, WISE, Herschel, Planck).

The SBNAF project makes **occultation predictions** for MBA events in 2017/18/19, as well as long- and short-term planning/calculations for TNO events. We also produce **high-quality images and fluxes** for NEAs, MBAs, and Centaurs/TNOs derived from Herschel photometric measurements. The new products are publically available from the Herschel Science Archive. We also support **asteroid-related calibration activities** for Herschel, ALMA, APEX, SOFIA, ISO, AKARI, IRAM, etc. calibration work.

4. Scientific results

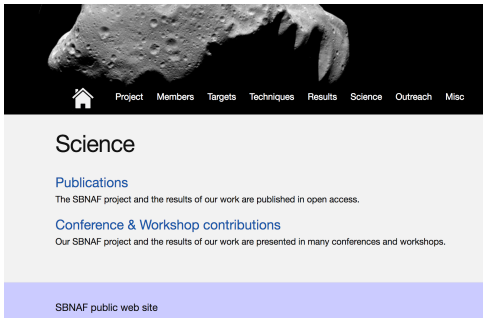

Figure 2: SBNAF web page where all SBNAF-related publications are documented and the open access links are provided.

Our SBNAF scientific results are documented in a large number of conference contributions and publications (see Figure 2). We are currently counting about 50 refereed publications (published, accepted, or submitted), with SBNAF contribution or led by SBNAF team members. The highlight publication is a Nature publication on "The size, shape, density and ring of the dwarf planet Haumea from a stellar occultation", by Ortiz et al. [2], which is based on a combined effort between the SBNAF and Lucky Star[1] teams, with inputs from many professional and amateur astronomers. The scientific SBNAF output is documented on our public web page at `http://www.mpe.mpg.de/~tmueller/sbnaf`. We will present selected results and highlights from our first two years of the SBNAF project.

Acknowledgements

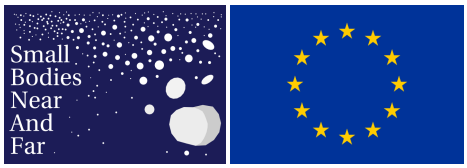

Figure 3: Left: The SBNAF project logo: `http://www.mpe.mpg.de/~tmueller/sbnaf/`. Right: The research leading to these results has received funding from the European Union's Horizon 2020 Research and Innovation Programme, under Grant Agreement no 687378.

References

[1] Müller, T. G., Marciniak, A., Kiss, C. et al. 2018: Small Bodies Near and Far (SBNAF): a benchmark study on physical and thermal properties of small bodies in the Solar System, accepted for publication by Advances in Space Research; `https://arxiv.org/abs/1710.09161`.

[2] Ortiz, J. L., Santos Sanz, P. Morales, N. et al. 2017: The size, shape, density and ring of the dwarf planet Haumea from a stellar occultation, Nature 550, 219-223.

[1] `http://lesia.obspm.fr/lucky-star/`